

Cite this: *Chem. Sci.*, 2020, **11**, 1848

All publication charges for this article have been paid for by the Royal Society of Chemistry

Transition metal-free catalytic reduction of primary amides using an abnormal NHC based potassium complex: integrating nucleophilicity with Lewis acidic activation†

Mrinal Bhunia, ‡ Sumeet Ranjan Sahoo, ‡ Arpan Das, Jasimuddin Ahmed, Sreejyothi P. and Swadhin K. Mandal*

An abnormal N-heterocyclic carbene (aNHC) based potassium complex was used as a transition metal-free catalyst for reduction of primary amides to corresponding primary amines under ambient conditions. Only 2 mol% loading of the catalyst exhibits a broad substrate scope including aromatic, aliphatic and heterocyclic primary amides with excellent functional group tolerance. This method was applicable for reduction of chiral amides and utilized for the synthesis of pharmaceutically valuable precursors on a gram scale. During mechanistic investigation, several intermediates were isolated and characterized through spectroscopic techniques and one of the catalytic intermediates was characterized through single-crystal XRD. A well-defined catalyst and isolable intermediate along with several stoichiometric experiments, *in situ* NMR experiments and the DFT study helped us to sketch the mechanistic pathway for this reduction process unravelling the dual role of the catalyst involving nucleophilic activation by aNHC along with Lewis acidic activation by K ions.

Received 25th November 2019
Accepted 26th December 2019

DOI: 10.1039/c9sc05953a

rsc.li/chemical-science

Introduction

Amines belong to a privileged class of compounds, routinely present in many fine and bulk chemicals, drugs, agrochemicals, dyes, surfactants, detergents and organic materials.^{1–6} One of the most attractive methods for synthesis of amines is the deoxygenative reduction of amides.⁷ However, the reduction of amides is the most challenging among all carboxylic derivatives because of their higher thermodynamic stability. The reduction of primary amides to primary amines is more stringent compared to secondary and tertiary amides.⁸

Among various synthetic methods to prepare primary amines such as reductive amination of carbonyls,^{9–15} borrowing hydrogenation methodologies,^{16–18} hydroamination of alkynes,^{19,20} reduction of nitriles,^{21–24} primary amides,²⁵ and carboxylic acids in the presence of ammonia,²⁶ reduction of primary amides is a straightforward route as amides are stable, naturally abundant, and inexpensive. Common methods for reduction of primary amides employing stoichiometric amounts of reactive metal hydride reagents such as lithium

aluminum hydride or sodium borohydrides are unattractive in terms of atom economy and environmental issues. In addition, they suffer from safety and selectivity of the process generating a stoichiometric amount of inorganic waste.⁷ In contrast, atom economical catalytic hydrogenation of primary amides is highly desirable and to date no example of catalytic hydrogenation of primary amides has been reported (Scheme 1).²⁶

As an alternative, catalytic hydrosilylation is an attractive approach for facile and efficient reduction of primary amides to amines.^{27–30} Earlier, Beller and coworkers utilized two different iron catalysts for efficient reduction of primary amides to primary amines in which the $[\text{NH}(\text{Et})_3][\text{Fe}_3\text{H}(\text{CO})_{11}]$ catalyst dehydrates primary amides to nitriles and the second catalyst $\text{Fe}(\text{OAc})_2$ was used for reduction of nitriles to the corresponding primary amines.²⁵ Very recently, our group has developed a single catalyst $[\text{Mn}^{\text{III}}(\text{O},\text{N},\text{N},\text{O}-\text{PLY})\text{Cl}]$ for hydrosilylation of primary amides into amines.³¹ Only a few examples of catalytic hydrosilylation of primary amides have been reported to date,^{25,31–33} while catalytic deoxygenative hydroboration of primary amides to amines has not been reported to date.

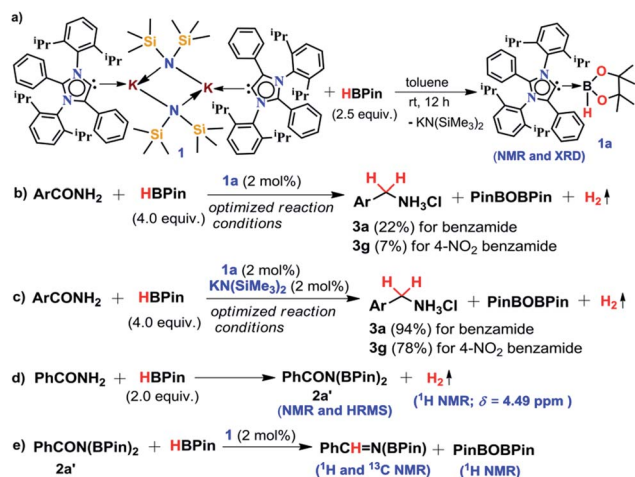
In the present study, we have achieved the reduction of primary amides to amines through deoxygenative hydroboration exploiting an abnormal N-heterocyclic carbene (aNHC) based potassium complex³⁴ (**1**) under ambient conditions in which the catalyst acts by integrating the nucleophilicity of weakly bound aNHC and Lewis acidic activation imparted by the K ions. It may be noted that to date a very few NHC-

Department of Chemical Sciences, Indian Institute of Science Education and Research Kolkata, Mohanpur-741246, India. E-mail: swadhin.mandal@iiserkol.ac.in

† Electronic supplementary information (ESI) available: Detailed experimental procedures, NMR and HRMS spectra, crystallographic details, and coordinates of the computed structures. CCDC 1900619. For ESI and crystallographic data in CIF or other electronic format see DOI: 10.1039/c9sc05953a

‡ M. Bhunia and S. R. Sahoo contributed equally to this work.





Scheme 3 A series of control experiments (a–e) conducted to understand the mechanistic pathway.

Å.⁵¹ Formation of **1a** in the reaction mixture in the presence of a borane establishes the role of **1** during catalysis. The weak ionic bond between K ion and aNHC in **1** as evident from the bond length (2.973 (2) Å)⁵⁴ makes the free aNHC available for adduct formation with borane. Thus **1** primarily acts as a carrier of aNHC during the catalytic reaction. Furthermore, to corroborate whether **1a** is an active catalyst or not, we accomplished the catalytic reduction of benzamide in the presence of 2 mol% **1a**, when benzamide and 4-nitrobenzamide offered only 22% and 7% yields of the corresponding phenylmethanamine hydrochloride salt, respectively, under the standard reaction conditions (Scheme 3b). On the other hand, the same reaction when performed with catalytic amounts of **1a** (2 mol%) and KN(SiMe₃)₂ (2 mol%), an excellent yield (94% for benzamide and 78% for 4-nitrobenzamide) of the reduction product was realized (Scheme 3c). However, only KN(SiMe₃)₂ failed to afford any reduction product (*vide supra*). These results clearly suggest that combination of KN(SiMe₃)₂ and aNHC is accountable for reduction of primary amides. Next, we performed the catalytic reduction of 4-nitrobenzamide in the presence of aNHC and different MN(SiMe₃)₂ (M = Na, and K), and scrutinized the relative yield. When KN(SiMe₃)₂ was used, it resulted in 78% yield while NaN(SiMe₃)₂ led to only 56% yield (Table S4, ESI[†]). This clearly indicates the role of alkali metal ions in the catalytic outcome of this reaction. To further investigate the reactivity difference between KN(SiMe₃)₂ and NaN(SiMe₃)₂, we undertook a density functional theory (B3LYP/6-31+g(2d,p)) analysis (Fig. 1). Optimized geometries clearly exhibited both the HOMO and HOMO–1 are primarily aNHC based (Fig. 1b), and a more destabilized HOMO (–8.3190 eV) and HOMO–1 (–9.0364 eV) for aNHC–KN(SiMe₃)₂ infers its better nucleophilicity towards borane (HBPIn) in comparison with the sodium analogue which in turn makes the B–H bond more nucleophilic upon adduct formation. Such adduct mediated nucleophilic activation of borane by aNHC has been reported in earlier studies.³⁸ Furthermore, when a catalytic amount of less nucleophilic

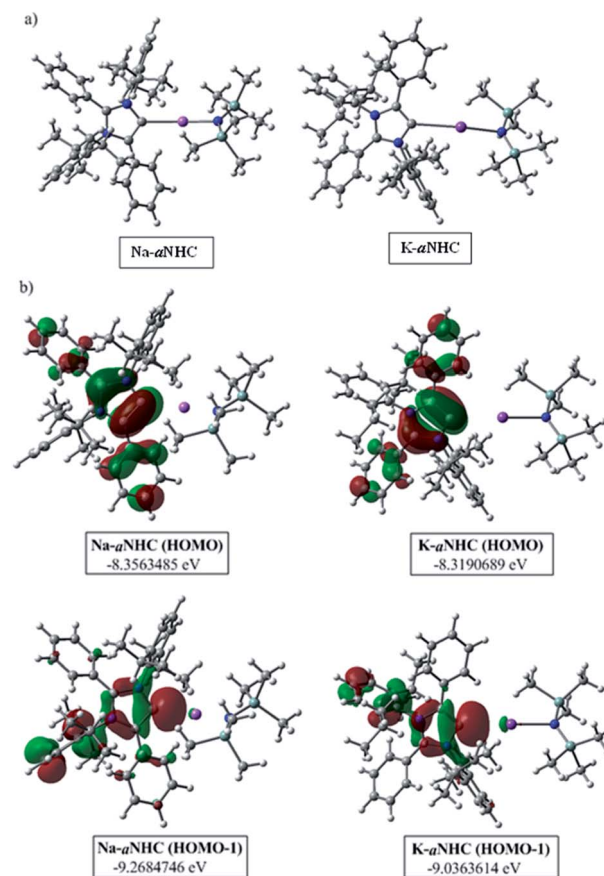


Fig. 1 (a) Optimized structures of aNHC–NaN(SiMe₃)₂ and aNHC–KN(SiMe₃)₂ complexes. (b) HOMO and HOMO–1 of the corresponding optimized species.

normal NHC (2.0 mol% IPr carbene) along with KN(SiMe₃)₂ (2.0 mol%) was used to reduce 4-nitrobenzamide, only 9% yield of the reduction product was realized (78% yield for **1**), suggesting the importance of higher nucleophilicity of aNHC in increasing the electron density on the boron center which promotes the nucleophilic addition of the B–H bond towards the carbonyl group of borylated amides (*vide supra*).⁵² Moreover, a stoichiometric reaction between benzamide and pinacolborane generates *N*-borylated amide (**2a'**), which was characterized through ¹H, ¹³C and ¹¹B NMR spectroscopic studies as well as mass spectrometry (Fig. S6–S8, ESI[†]). Notably, during the formation of *N*-borylated amide (**2a'**), evolution of hydrogen gas was monitored which was unambiguously supported by ¹H NMR resonance at δ 4.49 ppm (Scheme 3d).⁵³ Furthermore, a stoichiometric reaction was performed between *N*-borylated amide (**2a'**) and KN(SiMe₃)₂ to substantiate the role of KN(SiMe₃)₂. The sharp downfield shift of the carbonyl group (by 9.9 ppm) in the ¹³C NMR spectra (δ 179.1 ppm) compared to its borylated amide, **2a'** (δ 169.2 ppm) (Fig. S10, ESI[†]), clearly implies a Lewis acidic interaction between the K ion and carbonyl oxygen which was further supported by the DFT study (*vide infra*, Fig. 2b).⁵⁴ Such a Lewis acidic interaction may enhance the electrophilicity of amide carbonyl functionality. Furthermore, on treatment of catalyst **1** with borylated amide,





Scheme 4 Proposed catalytic cycle based on stoichiometric reactions.

2a', in the presence of HBPin and stopping the reaction prematurely after 2 h, partial formation of *N*-borylated imine was detected in the ^1H NMR spectrum at δ 10.34 ppm and in the ^{13}C NMR spectrum at δ 172.7 ppm in benzene- d_6 for benzamide (Fig. S12 and S13, ESI †). A similar reaction with 4-chlorobenzamide after 2 h exhibited the ^1H NMR resonance of the corresponding *N*-borylated imine (9) at δ 9.78 ppm (Fig. S14, ESI †) in toluene- d_8 (Scheme 3e).⁵⁵ Next, *N*-borylated imine, 9, reacts with HBPin in the presence of catalyst 1 to accomplish the reduced product *N*-diborylated amine (10) which was also characterized through ^1H , ^{13}C and ^{11}B NMR spectroscopy.²³

Based on these stoichiometric control experiments described above, a plausible mechanism for this transition metal-free reduction of primary amides is outlined in Scheme 4. In the first step, 1 reacts with pinacolborane to form 1a (X-ray) where the strong σ -donating property of aNHC increases the nucleophilicity to the B–H bond of borane (Fig. 2a). The organometallic K–aNHC complex acts as the carrier of aNHC which transfers the weakly bound aNHC to borane and generates $\text{KN}(\text{SiMe}_3)_2$. Next,

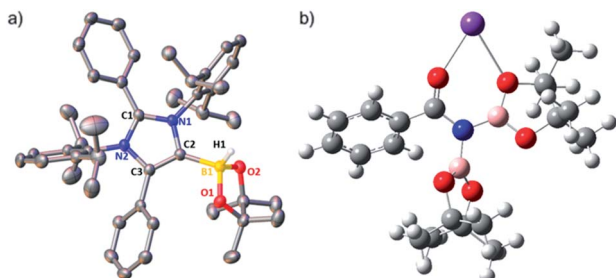


Fig. 2 (a) View of the molecular structure of 1a. Ellipsoids are set at the 50% probability level; hydrogen atoms except H1 of 1a have been omitted for the sake of clarity. (b) Computationally optimized structure of 7 at the B3LYP/6-31G* level of theory, showing interaction between the K ions and carbonyl oxygen.

$\text{KN}(\text{SiMe}_3)_2$ increases the electrophilicity of borylated amide, through Lewis-acidic interactions (evinced by NMR spectroscopy and the DFT calculated structure of 7, Fig. 2b).

On the other hand, the aNHC–borane adduct, 1a, reacts with activated borylated amide, 7, to form an intermediate borylated amine ester, 8. Strikingly, deoxygenative reduction of the carbonyl groups in isocyanate and formylated amines was carried out through hydroboration using alkaline earth metals which involved a similar hydride attack on carbonyl carbon to produce methylamine derivatives.^{56,57} Also, it may be noted that the borylated amide can be formed by the dehydrogenation reaction of benzamide and pinacolborane (as evidenced by stoichiometric experiments, see Scheme 3d) which is further activated by the *in situ* generated $\text{KN}(\text{SiMe}_3)_2$ through formation of 7 (DFT supported and ^{13}C NMR evidence). Next, elimination of a diboryl ether (authenticated by ^1H and ^{11}B NMR spectroscopies) leads to the formation of corresponding *N*-borylated imine, 9, which was also characterized by ^1H and ^{13}C NMR spectroscopies. The *N*-borylated imine next can undergo further reduction *via* another catalytic cycle (likewise cycle 1) to generate deoxygenative hydroborylated amine, 10, which was characterized through ^1H , ^{13}C and ^{11}B NMR spectroscopy and subsequent hydrolysis produces the corresponding primary amine.

Conclusions

In conclusion, we have demonstrated a transition metal-free catalytic reduction of primary amides to the corresponding primary amines using a well-defined aNHC based potassium complex through hydroboration. Notably, our reduction protocol exhibited a wide range of substrate scope including aromatic, heteroaromatic, and aliphatic primary amides. Moreover, this reduction methodology is considerably chemo-selective and applicable for chiral amides. Gram-scale production of phenylethylamine, a neuromodulator and neurotransmitter in the human CNS was also executed with this reduction strategy. Furthermore, with the help of a series of stoichiometric control experiments, *in situ* NMR experiments, X-ray crystallography and DFT study, we propose a mechanistic pathway for this challenging transformation where strong σ -donation of aNHC and labile character of organometallic K–aNHC were integrated with Lewis acidity imparted by *in situ* generated $\text{KN}(\text{SiMe}_3)_2$. Conceivably, the strong σ -donating properties of aNHC activated HBPin for nucleophilic addition of the B–H bond and the Lewis-acidic properties of $\text{KN}(\text{SiMe}_3)_2$ activated *in situ* generated borylated amide. Such a strategy of merging both nucleophilic and Lewis-acidic activation enables a transition metal free approach towards reduction of various primary amides.

Experimental section

General considerations

All manipulations were carried out using standard Schlenk techniques, high vacuum and also glovebox techniques below 0.1 ppm of O_2 and H_2O . All glassware were oven-dried at 130 $^\circ\text{C}$ and evacuated while hot prior to use. All solvents were distilled from Na/benzophenone prior to use. All other chemicals were



purchased from Sigma Aldrich and used as received. Elemental analyses were carried out using a PerkinElmer 2400 CHN analyzer and samples were prepared by keeping under a reduced pressure (10^{-2} mbar) overnight. The FT-IR spectra were recorded by transmission measurements of thin films with a PerkinElmer FT-IR spectrometer Spectrum RXI. The NMR spectra were recorded on a JEOL ECS 400 MHz spectrometer and on a Bruker Avance III 500 MHz spectrometer. All chemical shifts were reported in ppm using tetramethylsilane as a reference. Crystallographic data for structural analysis of **1a** (aNHC-HBPin adduct) were deposited at the Cambridge Crystallographic Data Center, CCDC number 1900619.

General method for reduction of primary amides

An oven dried 20 mL reaction tube was charged with [aNHC·KN(SiMe₃)₂]₂, **1** (14.8 mg, 2 mol%), and pinacolborane (290 μ L, 2.0 mmol, 4 equivalents) along with 1 mL toluene inside a N₂ filled glovebox. Next, primary amides (0.5 mmol, 1 equivalent) were added to the reaction mixture and stirred for 12 h at 40 °C. After completion of the reaction, 1.0 mL 2.0 (M) NaOH solution was added to the reaction mixture along with 1.0 mL Et₂O and stirred for another 1 h. Next, the reaction mixture was worked up with an Et₂O : H₂O mixture (1 : 1) and the corresponding reduced amines were concentrated in a vacuum. Consequently, 1.0 mL 1.0 (M) HCl was added to the concentrated amines followed by addition of 1.0 mL Et₂O and the corresponding amine hydrochloride salt was purified by washing with Et₂O. The isolated amine hydrochloride salts were characterized through NMR spectroscopy in DMSO-d₆.

Computational details

All theoretical calculations for geometry optimization and Natural Bonding Orbital (NBO) analysis of all the complexes were carried out with the help of Gaussian 16 (ref. 58) at the B3LYP level of theory by using the 6-31+g(2d,p) basis set.⁵⁹

X-ray crystallographic details

A single crystal of compound **1a** was mounted on a glass tip. Intensity data were collected on a SuperNova, Dual, Mo at zero, Eos diffractometer. The crystals were kept at 100 K during data collection. Atomic coordinates, isotropic and anisotropic displacement parameters of all the non-hydrogen atoms of two compounds were refined using Olex2,⁶⁰ and the structure was solved with the Superflip⁶¹ structure solution program using charge flipping and refined with the ShelXL⁶² refinement package using least squares minimization. Structure graphics shown in the figures were created using Olex2 and X-Seed software (version 2.0) packages.⁶³ Crystallographic data for structural analysis of **1a** were deposited at the Cambridge Crystallographic Data Center, CCDC number 1900619.

Conflicts of interest

There is no conflict to declare.

Acknowledgements

S. K. M. thanks SERB (DST), India (Grant No. EMR/2017/000772) for financial support. M. B. thanks Akamara Biomedicine Pvt. Ltd. for a research fellowship. S. R. S., A. D., and J. A. thank IISER Kolkata for a research fellowship. S. P. thanks DST, Inspire for a fellowship.

References

- 1 K. Weissmehl and H.-J. Arpe, *Industrial Organic Chemistry*, Wiley-VCH, Weinheim, 2008.
- 2 R. S. Vardanyan and V. J. Hruby, *Synthesis of Best-Seller Drugs*, Academic Press, Amsterdam, 2016.
- 3 S. A. Lawrence, *Amines: Synthesis, Properties and Applications*, Cambridge Univ. Press, Cambridge, 2004.
- 4 A. Gandini, T. M. Lacerda, A. J. F. Carvalho and E. Trovatti, *Chem. Rev.*, 2016, **116**, 1637–1669.
- 5 I. Delidovich, P. J. C. Hausoul, L. Deng, R. Pfütenreuter, M. Rose and R. Palkovits, *Chem. Rev.*, 2016, **116**, 1540–1599.
- 6 B. Chen, U. Dingerdissen, J. G. E. Krauter, H. G. J. L. Rotgerink, K. D. Möbus, J. Ostgard, P. Panster, T. H. Riermeier, S. Seebald, T. Tacke and H. Trauthwein, *Appl. Catal., A*, 2005, **280**, 17–46.
- 7 J. Seyden-Penne, *Reductions by the Alumino- and Boro-hydrides in Organic Synthesis*, John Wiley & Sons, Inc, New York, 1997.
- 8 L. Hie, N. F. F. Nathel, T. K. Shah, E. L. Baker, X. Hong, Y. F. Yang, P. Liu, K. N. Houk and N. K. Garg, *Nature*, 2015, **524**, 79–83.
- 9 S. Gomez, J. A. Peters and T. Maschmeyer, *Adv. Synth. Catal.*, 2002, **344**, 1037–1057.
- 10 J. L. Klinkenberg and J. F. Hartwig, *Angew. Chem., Int. Ed.*, 2011, **50**, 86–95.
- 11 G. Hahn, P. Kunnas, N. de Jonge and R. Kempe, *Nat. Catal.*, 2019, **2**, 71–77.
- 12 H. Alinezhad, H. Yavari and F. Salehian, *Curr. Org. Chem.*, 2015, **19**, 1021–1049.
- 13 L. Legnani, B. Bhawal and B. Morandi, *Synthesis*, 2017, **49**, 776–789.
- 14 A. Ruffoni, F. Juliá, T. D. Svejstrup, A. J. McMillan, J. J. Douglas and D. Leonori, *Nat. Chem.*, 2019, **11**, 426–433.
- 15 T. Senthamarai, K. Murugesan, J. Schneidewind, N. V. Kalevaru, W. Baumann, H. Neumanns, P. C. J. Kamer, M. Beller and R. V. Jagadeesh, *Nat. Commun.*, 2018, **9**, 4123–4134.
- 16 C. Gunanathan and D. Milstein, *Angew. Chem., Int. Ed.*, 2008, **47**, 8661–8664.
- 17 D. Pinggen, C. Müller and D. Vogt, *Angew. Chem., Int. Ed.*, 2010, **49**, 8130–8133.
- 18 S. Imm, S. Bähn, L. Neubert, H. Neumann and M. Beller, *Angew. Chem., Int. Ed.*, 2010, **49**, 8126–8129.
- 19 W. A. Herrmann, J. A. Kulpe, J. Kellner, H. Riepl, H. Bahrmann and W. Konkol, *Angew. Chem., Int. Ed. Engl.*, 1990, **29**, 391–393.
- 20 B. Zimmermann, J. Herwig and M. Beller, *Angew. Chem., Int. Ed.*, 1999, **38**, 2372–2375.



- 21 S. Enthaler, D. Addis, K. Junge, G. Erre and M. Beller, *Chem.-Eur. J.*, 2008, **14**, 9491–9494.
- 22 D. V. Gutsulyak and G. I. Nikonov, *Angew. Chem., Int. Ed.*, 2010, **49**, 7553–7556.
- 23 C. Weetman, M. D. Anker, M. Arrowsmith, M. S. Hill, G. Kociok-Köhn, D. J. Liptrot and M. F. Mahon, *Chem. Sci.*, 2016, **7**, 628–641.
- 24 S. Saha and M. S. Eisen, *ACS Catal.*, 2019, **9**, 5947–5956.
- 25 S. Das, B. Wendt, K. Möller, K. Junge and M. Beller, *Angew. Chem., Int. Ed.*, 2012, **51**, 1662–1666.
- 26 A. A. Núñez Magro, G. R. Eastham and D. J. Cole-Hamilton, *Chem. Commun.*, 2007, 3154–3156.
- 27 Y. Motoyama, K. Mitsui, T. Ishihda and H. Nagashima, *J. Am. Chem. Soc.*, 2005, **127**, 13150–13151.
- 28 S. Hanada, E. Tsutsumi, Y. Motoyama and H. Nagashima, *J. Am. Chem. Soc.*, 2009, **131**, 15032–15040.
- 29 S. Das, D. Addis, S. Zhou, K. Junge and M. Beller, *J. Am. Chem. Soc.*, 2010, **132**, 1770–1771.
- 30 Y. Sunada, H. Kawakami, T. Imaoka, Y. Motoyama and H. Nagashima, *Angew. Chem., Int. Ed.*, 2009, **48**, 9511–9514.
- 31 H. S. Das, S. Das, K. Dey, B. Singh, R. K. Haridasan, A. Das, J. Ahmed and S. K. Mandal, *Chem. Commun.*, 2019, **55**, 11868–11871.
- 32 M. Igarashi and T. Fuchikami, *Tetrahedron Lett.*, 2001, **42**, 1945–1947.
- 33 W. Yao, H. Fang, Q. He, D. Peng, G. Liu and Z. Huang, *J. Org. Chem.*, 2019, **84**, 6084–6093.
- 34 M. Bhunia, G. Vijaykumar, D. Adhikari and S. K. Mandal, *Inorg. Chem.*, 2017, **56**, 14459–14466.
- 35 P. L. Arnold, M. Rodden and C. Wilson, *Chem. Commun.*, 2005, 1743–1745.
- 36 R. W. Alder, M. E. Blake, C. Bortolotti, S. Bufali, C. P. Butts, E. Linehan, J. M. Oliva, A. G. Orpen and M. J. Quayle, *Chem. Commun.*, 1999, 241–242.
- 37 M. S. Hill, G. Kociok-Köhn and D. J. MacDougall, *Inorg. Chem.*, 2011, **50**, 5234–5241.
- 38 S. C. Sau, R. Bhattacharjee, P. K. Vardhanapu, G. Vijaykumar, A. Datta and S. K. Mandal, *Angew. Chem., Int. Ed.*, 2016, **55**, 15147–15151.
- 39 S. C. Sau, R. Bhattacharjee, P. K. Hota, P. K. Vardhanapu, G. Vijaykumar, R. Govindarajan, A. Datta and S. K. Mandal, *Chem. Sci.*, 2019, **10**, 1879–1884.
- 40 P. K. Hota, S. C. Sau and S. K. Mandal, *ACS Catal.*, 2018, **8**, 11999–12003.
- 41 A. Allen and R. Ely, *Synthetic methods for amphetamine*, www.nwafs.org/newsletters/SyntheticAmphetamine.pdf.
- 42 J. Chatterjee, F. Rechenmacher and H. Kessler, *Angew. Chem., Int. Ed.*, 2013, **52**, 254–269.
- 43 R. V. Jagadeesh, K. Murugesan, A. S. Alshammari, H. Neumann, M.-M. Pohl, J. Radnik and M. Beller, *Science*, 2017, **358**, 326–332.
- 44 G. Petranyi, N. S. Ryder and A. Stütz, *Science*, 1984, **224**, 1239–1241.
- 45 S. M. Nanavati and R. B. Silverman, *J. Am. Chem. Soc.*, 1991, **113**, 9341–9349.
- 46 M. Johannsen and K. Jørgensen, *Chem. Rev.*, 1998, **98**, 1689–1708.
- 47 K. Das, R. Shibuya, Y. Nakahara, N. Germain, T. Ohshima and K. Mashima, *Angew. Chem., Int. Ed.*, 2012, **51**, 150–154.
- 48 A. Ricci, in *Modern Amination Method*, Wiley-VCH, Weinheim, 2000.
- 49 B. M. Trost and M. L. Crawley, *Chem. Rev.*, 2003, **103**, 2921–2944.
- 50 T. Ohshima, Y. Miyamoto, J. Ipposhi, Y. Nakahara, M. Utsunomiya and K. Mashima, *J. Am. Chem. Soc.*, 2009, **131**, 14317–14328.
- 51 Crystal data for **1a**: C₄₅H₅₇BN₂O₂, Mr = 668.73, triclinic, space group *P* $\bar{1}$, *a* = 9.6381(5) Å, *b* = 11.4850(6), *c* = 19.0369(9) Å, α = 85.238(4)°, β = 75.946(4)°, γ = 75.838(5)°, *V* = 1981.44(18) nm³, *Z* = 4, ρ_{calc} = 1.121 g cm⁻³, μ (MoK α) = 0.513 mm⁻¹, *T* = 100(2) K, θ range for data collection = 4.786–131.826°, *R*₁ = 0.0529 (*I* > 2 σ (*I*)), w*R*₂ = 0.1208 (all data).
- 52 M. Bhunia, P. K. Hota, G. Vijaykumar, D. Adhikari and S. K. Mandal, *Organometallics*, 2016, **35**, 2930–2937.
- 53 M. Bhunia, S. R. Sahoo, B. K. Shaw, S. Vaidya, A. Pariyar, G. Vijaykumar, D. Adhikari and S. K. Mandal, *Chem. Sci.*, 2019, **10**, 7433–7441.
- 54 D. Mukherjee, S. Shirase, K. Mashima and J. Okuda, *Angew. Chem., Int. Ed.*, 2016, **55**, 13326–13329.
- 55 C. Boone, I. Korobkov and G. I. Nikonov, *ACS Catal.*, 2013, **3**, 2336–2340.
- 56 Y. Yang, M. D. Anker, J. Fang, M. F. Mahon, L. Maron, C. Weetman and M. S. Hill, *Chem. Sci.*, 2017, **8**, 3529–3537.
- 57 M. D. Anker, C. E. Kefalidis, Y. Yang, J. Fang, M. S. Hill, M. F. Mahon and L. Maron, *J. Am. Chem. Soc.*, 2017, **139**, 10036–10054.
- 58 M. J. Frisch, *et al.*, *Gaussian 09, Rev. D.01*, Gaussian, Inc., Wallingford, CT, 2010.
- 59 Y. Zhao and D. G. Truhlar, The M06 suite of density functionals for main group thermochemistry, thermochemical kinetics, noncovalent interactions, excited states, and transition elements: two new functionals and systematic testing of four M06-class functionals and 12 other functionals, *Theor. Chem. Acc.*, 2008, **120**, 215–241.
- 60 O. V. Dolomanov, L. J. Bourhis, R. J. Gildea, J. A. K. Howard and H. Puschmann, OLEX2: a complete structure solution, refinement and analysis program, *J. Appl. Crystallogr.*, 2009, **42**, 339–341.
- 61 L. Palatinus and G. Chapuis, SUPERFLIP, *J. Appl. Crystallogr.*, 2007, **40**, 786–790.
- 62 G. M. Sheldrick, SHELXL, *Acta Crystallogr., Sect. A: Found. Crystallogr.*, 2008, **64**, 112–122.
- 63 L. J. Barbour and *X-Seed: Graphical Interface to SHELX97 and POV-Ray*, University of Missouri-Columbia, Columbia, MO, 1999.

